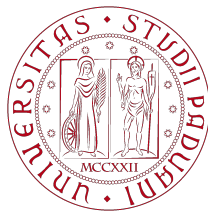


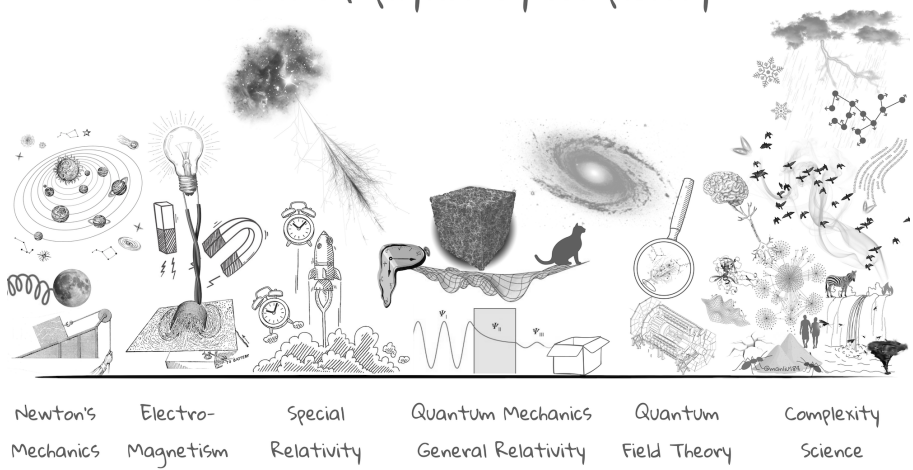
# Final Report

Physics of Complex Networks: Structure and Dynamics



UNIVERSITÀ  
DEGLI STUDI  
DI PADOVA

Areas of physics by complexity



## Projects Report: 15, 44

Tuscano Alessio

Last update: February 16, 2026

# Contents

---

<b>1</b>	<b>Task 15: Self-Organized Criticality on Networks</b>	<b>1</b>
1.1	Framework . . . . .	1
1.2	SOC on single topologies . . . . .	1
1.3	SOC with interdependence . . . . .	2
<b>2</b>	<b>Task 44: Social Connectedness Index II</b>	<b>4</b>
2.1	Dataset and network construction . . . . .	4
2.2	Completeness and weighted perspective . . . . .	4
2.3	Weighted clustering . . . . .	5
<b>3</b>	<b>Bibliography</b>	<b>7</b>

# 1 | Task 15: Self-Organized Criticality on Networks

---

## 1.1 | Framework

---

We simulate the Bak–Tang–Wiesenfeld (BTW) sandpile on a network with  $N$  nodes. Each node  $i$  carries an integer load  $z_i \in \{0, 1, 2, \dots\}$  and a threshold  $z_c(i)$ . At each driving step one grain is added to a uniformly random node; the system then relaxes via topplings. On a generic graph we set  $z_c(i) = k_i$  (degree threshold), so a toppling at  $i$  sends exactly one grain to each of its  $k_i$  neighbors:

$$z_i \leftarrow z_i - k_i, \quad z_j \leftarrow z_j + 1 \quad \forall j \in \partial i. \quad (1.1)$$

On finite networks without open boundaries, some form of dissipation is needed for a stationary state. We use *per-grain* dissipation [6]: each outgoing grain is independently lost with probability  $f$ , so that on average a fraction  $f$  of the redistributed load disappears per toppling. An *avalanche* is the full relaxation triggered by one grain addition. We measure: size  $S$  (total topplings), duration  $T$  (parallel-update waves), and area  $A$  (distinct toppled nodes).

## 1.2 | SOC on single topologies

---

**Mean-field baseline (Bonabeau).** In the random-neighbor (annealed) model [2] each toppling redistributes grains to  $k$  nodes chosen uniformly at random rather than along fixed edges. This removes quenched structural correlations and yields mean-field exponents: the avalanche-size distribution follows  $P(S) \sim S^{-3/2}$ , i.e. the CCDF scales as  $P(S \geq s) \sim s^{-1/2}$ . We verify this numerically with  $N = 20\,000$ ,  $k = 4$ , and dissipation  $\varepsilon \in \{10^{-3}, 3 \times 10^{-3}, 10^{-2}\}$  ( $3 \times 10^5$  driving steps each,  $2 \times 10^4$  transient discarded). Fig. 1.1 (left) confirms the expected power-law tail; smaller  $\varepsilon$  extends the scaling regime before the finite-size cutoff.

**Quenched scale-free topology (Goh et al.).** On a quenched scale-free network generated with the static model [6] (mean degree  $\langle k \rangle = 4$ , degree threshold  $z_c(i) = k_i$ ), the avalanche exponent depends on the degree exponent  $\gamma$ . Goh et al. predict  $\tau_A = \gamma/(\gamma - 1)$  for  $2 < \gamma < 3$  (non-mean-field) and  $\tau_A = 3/2$  for  $\gamma \geq 3$  (mean-field), with  $\tau_A$  defined via  $P(A) \sim A^{-\tau_A}$ .

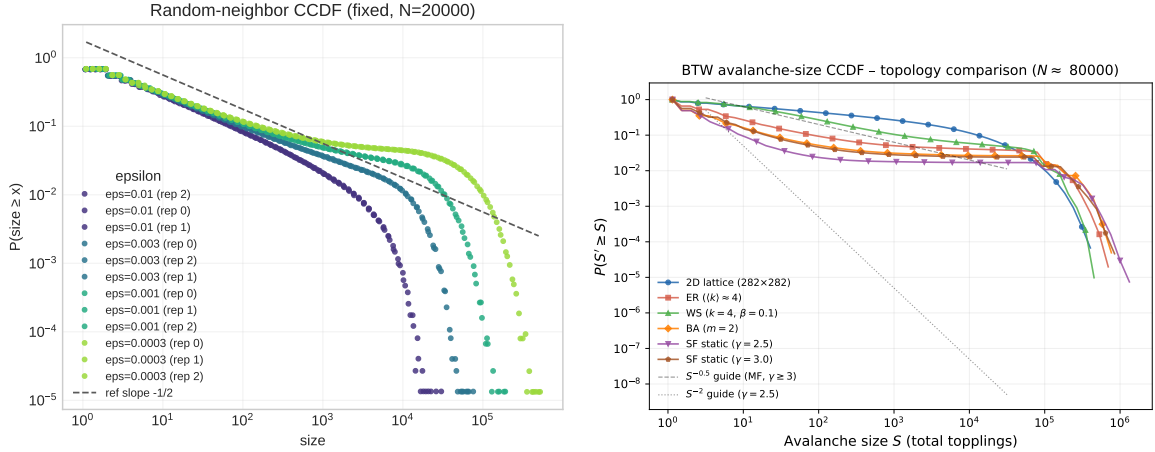


Figure 1.1: Left: annealed random-neighbor model ( $N = 20\,000$ ,  $k = 4$ ) avalanche-size CCDF for three dissipation rates; dashed line marks the mean-field slope  $-1/2$ . Right: avalanche-size CCDF on six quenched topologies ( $N \approx 80\,000$ , degree threshold,  $f = 10^{-4}$ ); homogeneous networks cluster near the MF guide while heterogeneous ones (BA, SF) show progressively steeper tails.

**Topology comparison.** We run the BTW sandpile ( $z_c(i) = k_i$ , per-grain dissipation  $f = 10^{-4}$ ,  $5 \times 10^5$  steps,  $5 \times 10^4$  transient) on six synthetic topologies with  $N \approx 80\,000$ : a 2D square lattice ( $282 \times 282$ , open boundary), an Erdős–Rényi (ER) random graph ( $\langle k \rangle \approx 4$ ), a Watts–Strogatz (WS) small-world network ( $k = 4$ , rewiring  $\beta = 0.1$ ), a Barabási–Albert (BA) preferential-attachment network ( $m = 2$ ), and two scale-free (SF) networks from the static model with  $\gamma = 2.5$  and  $\gamma = 3.0$ . Fig. 1.1 (right) overlays the resulting avalanche-size CCDFs. The homogeneous topologies (lattice, ER, WS) cluster near the mean-field  $S^{-1/2}$  guide, confirming that low degree variance leaves scaling unaffected. In contrast, the heterogeneous networks (BA, SF) should show markedly steeper tails: degree-heterogeneity concentrates load on hubs, producing more frequent moderate cascades but suppressing the very large ones. The SF static model with  $\gamma = 2.5$  matches the predicted  $\tau_S = \gamma/(\gamma - 1) = 5/3$  exponent ( $\text{CCDF} \sim S^{-2/3}$ , much steeper than MF), while  $\gamma = 3.0$  already approaches the MF regime [6]. While slightly different from what expected for heterogeneous topologies, we get a qualitatively consistent pattern of for more heterogeneous networks, with a consistent pattern but not in the  $S^{-2}$  regime.

### 1.3 | SOC with interdependence

**Coupled sandpiles and large cascades.** We now consider two modules  $A$  and  $B$ , each with  $N = 2000$  nodes, connected by a sparse set of inter-module edges (bridges). Each node in module  $A$  is independently selected as a bridge endpoint with probability  $p$ ; the same number of nodes is drawn from  $B$  and paired uniformly at random [3]. Because the threshold is degree-based, adding a bridge to node  $i$  raises its threshold  $z_c(i)$  by one (higher local stability), but also creates a new pathway for load to propagate between modules.

Following [3], we classify events by whether a *large* cascade occurs in module  $A$ :  $S_A > C$  with  $C = N/2 = 1000$ . We also track *global* cascades ( $S > C_g$ ,  $C_g = N =$

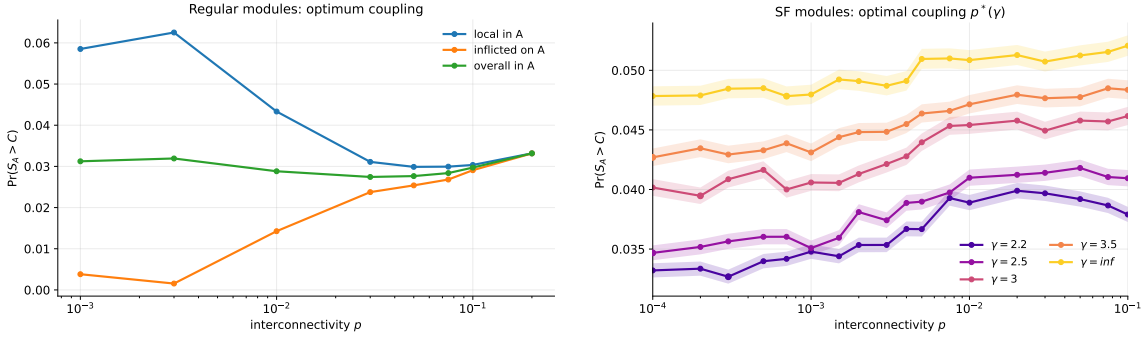


Figure 1.2: Probability of a large cascade in module  $A$  versus coupling  $p$ . Left: regular modules ( $z = 3$ ) showing the local/inFLICTed/overall decomposition. Right: SF modules for several  $\gamma$ ; lower  $\gamma$  shifts the minimum to smaller  $p$ .

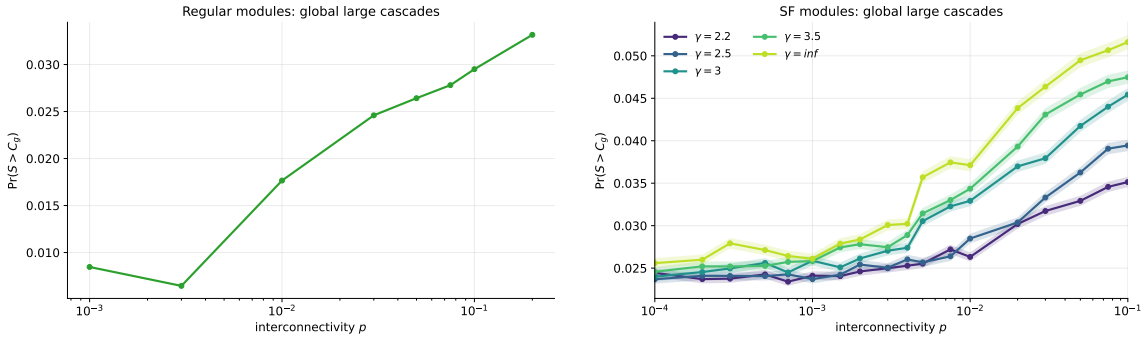


Figure 1.3: Probability of a *global* large cascade ( $S > C_g = 2000$ ) versus  $p$ . The non-monotonic shape persists, supporting the “optimal coupling” interpretation rather than a cutoff artifact.

2000). Dissipation is per-toppling with  $f = 0.01$ ; each simulation runs  $5 \times 10^5$  steps with  $5 \times 10^4$  transient. The “regular” modules are random 3-regular graphs; the scale-free modules use the static model with tunable  $\gamma$  (taking  $\gamma = \infty$  recovers a homogeneous degree distribution near the ER limit). In the SF panels, shaded bands show 95% Wilson-score confidence intervals from aggregated event counts across 2 replicates.

Fig. 1.2 separates cascades that remain within  $A$  (local) from those triggered by activity arriving from module  $B$  (inflicted), and their union (any large in  $A$ ). At small  $p$ , the few bridges divert load away from module  $A$ , suppressing its largest within-module cascades. At large  $p$ , bridges raise node thresholds (making individual topplings less frequent) but simultaneously enable inflicted cascades: when a node does topple, it can inject load into the other module. The competition between these two effects can produce a non-trivial optimum  $p^*$  at which large cascades are least likely [3].

Global cascades (Fig. 1.3) show the same qualitative non-monotonic pattern. Small coupling suppresses the largest events; strong coupling enables system-wide propagation. For the regular-module case, the optimum lies near  $p^* \approx 0.01$ , consistent with [3]. In the SF extension, the optimum  $p^*$  shifts to smaller values for lower  $\gamma$ : heterogeneous networks are more sensitive to inter-module coupling, likely because high-degree hubs act as efficient conduits for cross-module load transfer once bridges reach them.

## 2

# Task 44: Social Connectedness Index II

---

## 2.1

### Dataset and network construction

---

The Social Connectedness Index (SCI) by Meta quantifies the intensity of Facebook friendship ties between pairs of administrative regions [1]. For regions  $i, j$  the published score is

$$\text{SCI}_{ij} \propto \frac{F_{ij}}{U_i U_j},$$

where  $F_{ij}$  counts cross-region friendships and  $U_i, U_j$  are the Facebook-user populations; values are rescaled within each layer to  $[1, 10^9]$  (`scaled_sci`) [7]. We use the SCI II release (reference period 2025-12-26 to 2026-01-25, CC0) [7] and, following task instructions, exclude the USA.

**Resolution.** We adopt the finest resolution available in the SCI layer files: **NUTS 3** for EU countries (via GISCO 2024 boundaries [4]) and **GADM level 1** for all others (GADM v4.1 [5]). The SCI data do not provide sub-national codes at GADM level 3; GADM 1 is therefore the highest resolution accessible outside Europe.

**Construction.** From the raw layer CSVs we retain only *within-country* edges, drop self-loops, keep one edge per unordered pair, and sum duplicate `scaled_sci` values. Geographic coordinates (EPSG:4326) are obtained from boundary-polygon representative points. The resulting global deliverable contains  $N = 3\,040$  nodes and  $E = 134\,016$  edges across 99 countries; coordinate coverage is  $\sim 98\%$  of nodes.

## 2.2

### Completeness and weighted perspective

---

A key observation is that *every* within-country graph is **complete**: the SCI dataset reports a weight for every pair of regions, so  $E = \binom{N}{2}$  and density = 1 for all 99 countries (Fig. 2.1, left). Consequently, standard unweighted metrics are uninformative:  $P(k) = \delta_{k,N-1}$ ,  $C = 1$ , and modularity  $Q = 0$ . All meaningful structure resides in the *weights*; the remainder of the analysis is therefore weighted.

**Edge-weight distribution.** Within each country we normalise weights by the maximum ( $\hat{w}_{ij} = w_{ij}/w_{\max}$ ) and pool all edges across the 99 countries. The resulting

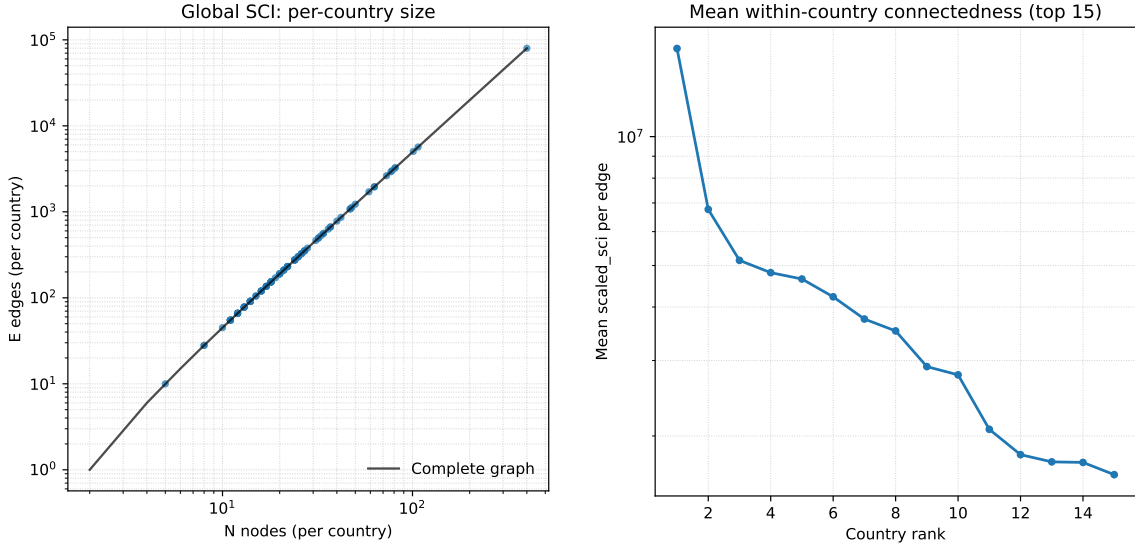


Figure 2.1: Left: edges versus nodes per country (log–log); the black curve is the complete-graph reference  $E = N(N - 1)/2$ , confirming density = 1 for all countries. Right: mean within-country `scaled_sci` per edge versus country rank (top 15).

CCDF (Fig. 2.2, left) spans roughly four decades with a heavy tail: most edges carry low relative weight while a few region pairs are orders of magnitude more connected.

**Node strength and Gini coefficient.** The strength of node  $i$  is  $s_i = \sum_j w_{ij}$ . We summarise within-country strength heterogeneity via the Gini coefficient  $G \in [0, 1]$  (Fig. 2.2, right). Values range from  $G \approx 0.07$  (Japan, very homogeneous) to  $G \approx 0.35$  (UK, dominated by London); the colour encodes mean strength, showing that heterogeneity is not simply a size effect.

## 2.3 | Weighted clustering

For complete graphs the unweighted clustering coefficient is trivially 1. We therefore compute the *weighted* clustering of Onnela et al. [8]:

$$C_i^w = \frac{1}{s_i(k_i - 1)} \sum_{j,h} (\hat{w}_{ij} \hat{w}_{ih} \hat{w}_{jh})^{1/3},$$

where  $\hat{w}$  is the max-normalised weight.  $C^w$  equals 1 only when all triangle weights are identical (perfectly homogeneous connectivity); heterogeneous weights lower it.

Fig. 2.3 (left) shows  $\langle C^w \rangle$  per country (computed for countries with  $N \leq 120$  for tractability). Russia, Japan, and Uganda ( $C^w \gtrsim 0.89$ ) exhibit nearly uniform regional connectivity, whereas the UK ( $C^w \approx 0.39$ ) is strongly London-centric. The weight matrix of Italy (Fig. 2.3, right) visualises the block structure typical of countries with a few dominant metropolitan areas.

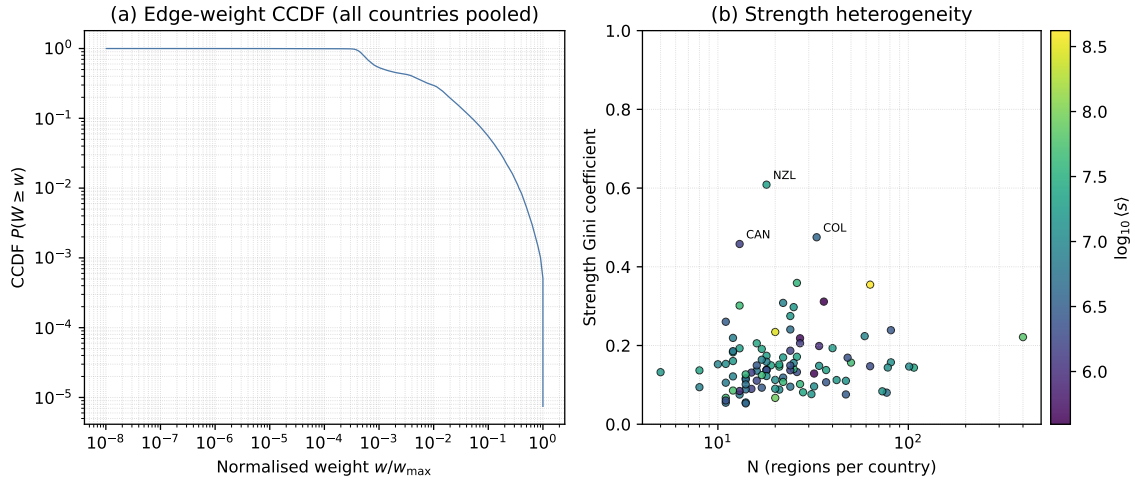


Figure 2.2: Left: CCDF of the max-normalised edge weight pooled across all 99 countries. Right: strength Gini coefficient versus network size; colour indicates  $\log_{10}\langle s \rangle$ .

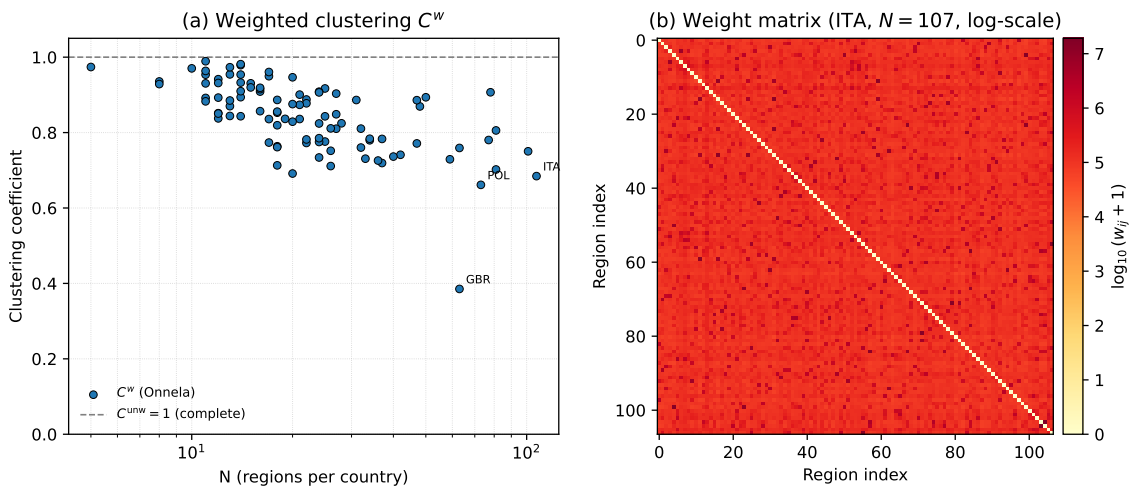


Figure 2.3: Left: weighted clustering  $\langle C^w \rangle$  versus  $N$ ; dashed line marks  $C^{\text{unw}} = 1$ . Right: log-scaled weight matrix for Italy ( $N = 107$ , NUTS3 regions).

## 3 | Bibliography

---

- [1] AI and Data for Good at Meta. Social connectedness index. <https://ai.meta.com/ai-for-good/datasets/social-connectedness-index/>, 2026. [Accessed 04-Feb-2026]. Reference period: 2025-12-26 to 2026-01-25. Updated: 2026-01-29.
- [2] Eric Bonabeau. Sandpile dynamics on random graphs. *Journal of the Physical Society of Japan*, 64(9):327–336, 1995. doi: 10.1143/JPSJ.64.327.
- [3] Charles D. Brummitt, Raissa M. D’Souza, and E. A. Leicht. Suppressing cascades of load in interdependent networks. *Proceedings of the National Academy of Sciences*, 109(12):E680–E689, 2012. doi: 10.1073/pnas.1110586109.
- [4] European Commission, Eurostat (GISCO). Nuts regions (2024) - gisco distribution (level 3, epsg:4326). <https://gisco-services.ec.europa.eu/distribution/>, 2024. [Accessed 04-Feb-2026]. GeoJSON endpoint used: NUTS\_RG\_01M\_2024\_4326\_LEVL\_3.
- [5] GADM. Gadm database of global administrative areas (version 4.1). <https://gadm.org/>, 2025. [Accessed 04-Feb-2026]. Shapefile downloads mirrored at <https://geodata.ucdavis.edu/gadm/>.
- [6] K.-I. Goh, D.-S. Lee, B. Kahng, and D. Kim. Sandpile on scale-free networks. *Physical Review Letters*, 91:148701, 2003. doi: 10.1103/PhysRevLett.91.148701.
- [7] Humanitarian Data Exchange (HDX). Facebook social connectedness index. <https://data.humdata.org/dataset/social-connectedness-index>, 2026. [Accessed 04-Feb-2026]. Coverage: 178 countries. Reference period: 2025-12-26 to 2026-01-25. Updated: 2026-02-07. License: CC0.
- [8] J.-P. Onnela, J. Saramäki, J. Kertész, and K. Kaski. Intensity and coherence of motifs in weighted complex networks. *Physical Review E*, 71:065103, 2005. doi: 10.1103/PhysRevE.71.065103.